ACS APPLIED MATERIALS & INTERFACES

Research Article

www.acsami.org

One-Pot Construction of Functional Mesoporous Silica Nanoparticles for the Tumor-Acidity-Activated Synergistic Chemotherapy of Glioblastoma

Ze-Yong Li, Yun Liu, Xiao-Qiang Wang, Li-Han Liu, Jing-Jing Hu, Guo-Feng Luo, Wei-Hai Chen, Lei Rong, and Xian-Zheng Zhang*

Key Laboratory of Biomedical Polymers of the Ministry of Education & Department of Chemistry, Wuhan University, Wuhan 430072, P. R. China

Supporting Information

ABSTRACT: Mesoporous silica nanoparticles (MSNs) have proved to be an effective carrier for controlled drug release and can be functionalized easily for use as stimuli-responsive vehicles. Here, a novel intelligent drug-delivery system (DDS), camptothecin (CPT)-loaded and doxorubicin (DOX)-conjugated MSN (CPT@MSN-hyd-DOX), is reported via a facile one-pot preparation for use in synergistic chemotherapy of glioblastoma. DOX was conjugated to MSNs via acid-labile hydrazone bonds, and CPT was loaded in the pores of the MSNs. At pH 6.5 (analogous to the pH in tumor tissues), a fast DOX release was observed that was attributed to the hydrolysis of the hydrazone bonds. In addition, a further burst release of DOX was found at pH 5.0 (analogous to the pH in lyso/endosomes of tumor cells), leading to a strong synergistic effect. In all, CPT and DOX could be delivered simultaneously into tumor cells, and this intelligent DDS has great potential for tumor-trigged drug release for use in the synergistic chemotherapy of tumors.

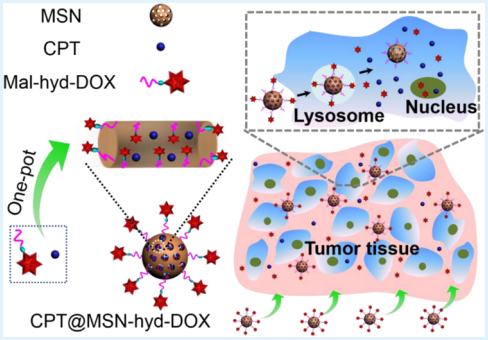

KEYWORDS: *mesoporous silica nanoparticle, drug release, tumor-acidity-activate, synergistic chemotherapy*

INTRODUCTION

Glioblastoma is the most common and aggressive malignant primary brain tumor in humans and a challenging disease to treat.[1] Chemotherapy alone or a combination with radiation therapy is still the standard treatment after maximal safe surgical resection, but the therapeutic effect remains quite poor despite some advances[2] because of insufficient drug dosage to the diseased regions. To sweep out the obstacles for the effective chemotherapy of glioblastoma, combination chemotherapy has attracted increasing attention because of its enhanced therapeutic efficiency as compared with the unsatisfactory results of single agents in the treatment of advanced tumors.[3,4] To date, the aim for combination chemotherapy has focused on attacking different biochemical targets and circumventing drug resistance in heterogeneous tumors.[4] The general principle of combination chemotherapy is to use drugs with independent mechanisms of action and to deliver multiple drugs at their maximum tolerated dose as early as possible in the disease. In this regard, many antitumor drugs without overlapping toxicities and cross-resistance were used together to afford a remarkable synergistic effect for enhanced cancer cell killing. Among them, combining CPT with DOX is an excellent combination that has been frequently used.[5,6] Both CPT and DOX are DNA-damaging drugs that result in the unwinding of DNA for transcription by inhibiting the progression of the topoisomerase I (CPT) and II (DOX)[7] enzymes to enhance the DNA-damaging efficiency.

In cancer treatment, drug-delivery systems (DDSs), which can overcome the rapid blood clearance and severe side effects of chemotherapeutics, enhance the water solubility of the drugs, and achieve tumor selectivity, are of significant importance. Various nanosized DDSs, including liposomes, nanogels, polymeric nanoparticles, inorganic nanoparticles, and nanomicelles were developed to deliver anticancer drugs to tumor tissues via the enhanced permeation and retention (EPR) effect. Among these systems, the use of MSNs as a drug carrier[8−10] has attracted considerable interest in recent years, owing to their high specific surface area, uniform porosity, large pore volume, easy postsynthesis, and good biocompatibility. Recently, intelligent DDSs based on MSNs were also reported.[11−18] Among them, pH-triggered drug-delivery systems, which can response to different pH values in different microenvironments, are the most frequently investigated ones. As we know, the cellular compartments in tumor tissues are more acidic (pH 5.8−7.1)[19] than that in normal tissues (pH 7.4), and the pH of endo/lysosomes is even lower at 5.0−5.5.[20] By utilizing these differences in pH values, a number of pH-

Received: May 30, 2013
Accepted: July 19, 2013
Published: July 19, 2013

responsive delivery vehicles based on MSNs have been developed for pH-triggered drug delivery.[15,17,21−24] Zink and co-workers designed several MSN-based nanocarriers that kept drug molecules encapsulated at neutral conditions but released them when the pH was less than 6.0.[15,23] Apparently, those smart nanocarriers were designed for endo/lysosomal pH-responsive drug delivery. Persistent efforts have been made to develop a new strategy for tumor-targeting or tumor-triggered targeted drug delivery.[25] The strategy centers on constructing nanocarriers that could maintain their "stealth" function in blood circulation and then transform into a more cell-interactive form to show tumor-triggered drug release or enhanced interaction between the nanocarriers and tumor cells in a tumor-specific manner.[26]

Herein, we report the synthesis and construction of a pH-responsive, MSN-based dual-drug-delivery system, CPT@MSN-hyd-DOX, where CPT was physically loaded into MSN with chemically conjugated DOX via an acid-labile hydrazone bond. As shown in Scheme 1, the delivery system has following

Scheme 1. CPT@MSN-hyd-DOX As a Functional Dual-Drug-Delivery System for the Tumor-Acidity-Activated Synergistic Chemotherapy of Glioblastoma

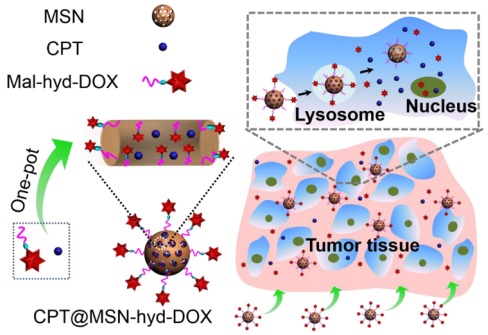

features: (a) the nanoparticles can be conveniently and easily constructed via a facile one-pot strategy, (b) the acid-labile hydrazone bond for DOX conjugation is extraordinarily sensitive to the slightly acidic tumor extracellular environment (i.e., the nanoparticles can maintain a relatively "stealth" status during circulation and release DOX triggered by the tumor acidity when they accumulate at the tumor site via the EPR effect), (c) as a hydrophobic antitumor drug, CPT loaded in the pores of MSNs can be effectively delivered to tumor cells with a sustained release,[27] and (d) the conspicuous synergistic effect of CPT and DOX can be activated by tumor acidity and further promoted by the increased acidity in subcellular compartments such as the lyso/endosomes.

EXPERIMENTAL SECTION

Materials. *N*-cetyltrimethylammonium bromide (CTAB) and tetraethylorthosilicate (TEOS) were purchased from Shanghai Reagent Chemical Co. (China). Doxorubicin hydrochloride was provided by Zhejiang Hisun Pharmaceutical Co. (China). 3-Mercaptopropyltrimethoxysilane, 3-isocyanatepropyltriethoxysilane, and camptothecin were obtained from Aladdin Reagent Co. Ltd. (Shanghai, China). The sulfhydryl-reactive (6-maleimidocaproyl)-hydrazone of doxorubicin was synthesized according to a previous report.[28] alpha-Modified Minimum Essential Medium (alpha-MEM), fetal bovine serum (FBS), Dulbecco's phosphate buffered saline (PBS), 3-[4,5-dimethylthiazol-2-yl]-2,5-diphenyltetrazolium-bromide (MTT), Hochest 33342, LysoSensor Green DND-189, and Hoechst S769121 trihydrochloride trihydrate (nuclear yellow) were purchased from Invitrogen. All other reagents and solvents were provided by the Shanghai Reagent Chemical Co. (China) and used as received.

Methods. ^{1}H NMR spectra were recorded on a Mercury VX-300 spectrometer (Varian) at 300 MHz. FT−IR spectra were recorded on an AVATAR 360 spectrometer. Thermal gravimetric analysis (TGA) was performed on a TGS-2 thermogravimetric analyzer (PerkinElmer). Fluorescence spectra were recorded on a RF-5301PC spectrofluorophotometer (Shimadzu). Transmission electron microscopy (TEM) was carried out with a JEM-2100 instrument. Surface area was obtained by the Brunauer−Emmett−Teller (BET) approach, and the pore-size distributions were calculated by the Barrett−Joyner−Halenda method (ASAP2020, Micromeritics).

Synthesis of MSN. MSN was synthesized by the following procedure: NaOH (0.28 g) and CTAB (1.00 g) were dissolved in 480 mL of deionized water and heated to 80 °C. TEOS (5.00 mL) was then added dropwise to the solution. The mixture was allowed to stir for 2 h to produce a white precipitate. Finally, the solid product was centrifuged, washed with deionized water and methanol, and dried under high vacuum. To remove the surfactant template (CTAB), the white solid was refluxed for 24 h in a solution of 1.0 mL of HCl (37%) and 80.0 mL of methanol, washed extensively with deionized water and methanol, and vacuum-dried.

Synthesis of 3-Mercaptopropyl-Functionalized MSN (MSN-SH). MSN (100 mg) in methanol (20 mL) was functionalized with 5 mL of 3-mercaptopropyltrimethoxysilane at room temperature for 24 h to produce MSN-SH nanoparticles. The particles were separated by centrifugation (9000 rpm, 10 min), washed five times with methanol, and dried under vacuum overnight.

Synthesis of 3-Isocyanatopropyl-Functionalized MSN (MSN-NCO). MSN (100 mg) was refluxed for 24 h in 20 mL of anhydrous toluene with 2 mL of 3-isocyanatopropyltriethoxysilane under an N_2 atmosphere, washed with anhydrous toluene and anhydrous tetrahydrofuran (THF), and dried under vacuum to yield MSN-NCO.

Synthesis of DOX-Conjugated MSN via Urea Linkers (MSN-urea-DOX) and Hydrazone Bonds (MSN-hyd-DOX). MSN-NCO (50 mg) was added to anhydrous dimethylformamide (DMF, 5 mL). DOX (10 mg) and 4-methylmorpholine (NMM, 6 μL) were then added to the solution. The solution was stirred in the dark for 24 h at 60 °C to yield MSN-urea-DOX. The resulting material was centrifuged and washed thoroughly with DMF and methanol and dried under high vacuum. MSN-hyd-DOX was prepared simply by Mal-hyd-DOX reacting with MSN-SH in a dark environment at room temperature for 24 h.

Preparation of CPT-loaded MSN (CPT@MSN) as well as CPT-loaded and DOX-conjugated MSN via Urea Linkers (CPT@MSN-urea-DOX) and Hydrazone Bonds (CPT@MSN-hyd-DOX). Into 10 mL DMF were added 20 mg of CPT, 30 mg of Mal-hyd-DOX, and 100 mg of MSN-SH, and the suspension was sonicated for 30 min. After stirring in the dark for 24 h under an N_2 atmosphere, DOX-conjugated and CPT-loaded nanoparticles were obtained. The nanoparticles were centrifuged (8000 rpm, 10 min), washed thoroughly with CPT-saturated water and methanol, and dried under vacuum to yield red solidified CPT@MSN-hyd-DOX. CPT@MSN and CPT@MSN-urea-DOX were prepared according to the same steps described earlier.

In Vitro Release Studies. In vitro release experiments were carried out at pH values of 7.4, 6.5, and 5.0 using 50 mM Na_2HPO_4−NaH_2PO_4, Na_2HPO_4−NaH_2PO_4, and CH_3COONa−CH_3COOH buffer solutions, respectively. For each release study, 10 mg of nanoparticles were suspended in 3 mL of buffer solution, and the solution was put into a dialysis tube that was directly immersed into 40 mL of buffer solution and maintained at 37 °C. The concentrations of the released drugs were calculated by the measurement of the fluorescence intensity (λ_{ex} = 488 nm for DOX and λ_{ex} = 365 nm for CPT) with reference to the standard curve. After each sampling, the buffer solution was refreshed immediately.

In Vitro Cytotoxicity. In vitro cytotoxicity of human glioblastoma astrocytoma (U87 MG) cells under different treatments was performed using the MTT assay. For the cell death assay under normal physiological pH conditions, the cells were cultured in a 96-

well dish (6000 cells/well) with 200 μL alpha-MEM containing 10% FBS. After incubation (37 °C and 5% CO_2) for 24 h, the culture media in each well was replaced with 200 μL of fresh alpha-MEM containing the drugs in DMSO, MSN, or drug-loaded MSNs in PBS at the indicated concentrations. The incubation of each material was continued for 48 h. Next, the media was refreshed with alpha-MEM and 20 μL of the MTT solution (5 mg mL^{-1}). After incubation for 4 h, 200 μL of DMSO was added to each well, and the plate was shaken at room temperature. The optical density (OD) was measured with a microplate reader (BIO-RAD, Model550, USA) at 570 nm. The viability was calculated by the following equation: cell viability = $OD_{570(treated)}/OD_{570(control)}$, where $OD_{570(treated)}$ was obtained in the presence of the drugs or nanoparticles.

For the cell death assay at the indicated pH values, the cells were cultured in a 96-well dish (6000 cells/well) with 200 μL of alpha-MEM containing 10% FBS. After incubation for 24 h, the culture media of some wells was replaced with fresh culture media (200 μL) at pH 6.5 and others were replaced with fresh culture media (200 μL) at pH 7.4. The fresh culture media at both pH values contained CPT@MSN-hyd-DOX at different DOX doses. After a 4 h incubation, the culture media of all wells was refreshed with culture media (200 μL) at pH 7.4 and further incubated for 48 h. After that, MTT was utilized to determine the cell viability.

Confocal Laser-Scanning Microscopy. To visualize the intracellular uptake and drug release of CPT@MSN-hyd-DOX and CPT@MSN-urea-DOX, U87 MG cells were cultured in 35 mm Petri dishes. The cells were incubated with nanoparticles in serum-free media at an equivalent DOX concentration of 2.36 μg mL^{-1} (2.65 μg mL^{-1} for CPT) for 2 or 4 h at 37 °C in the dark. The cells were washed twice with PBS and stained with 1 μM LysoSensor Green DND-189, Hoechst 33342, and Nuclear Yellow for 15 min in the dark. Prior to imaging via confocal microscopy (NOL-LSM 710), the cells were washed thrice with PBS and transferred into serum-free media.

RESULTS AND DISCUSSION

Preparation and Characterization of CPT@MSN-hyd-DOX. The sulfhydryl-reactive (6-maleimidocaproyl)hydrazone of DOX (Mal-hyd-DOX) was initially synthesized according to the literature,[28] and the synthetic route is illustrated in Scheme S1 in the Supporting Information. ^1H NMR was utilized to monitor the synthesis process (Figures S1–S3), and the product, Mal-hyd-DOX, was further confirmed by ESI–MS (Figure S4). Next, the MCM-41-type template-removed mesoporous silica nanoparticle (MSN) was synthesized according to a reference procedure,[13] and the direct evidence for the formation of MSN was provided by TEM images. As shown in Figure 1a, the diameter of MSN was around 140 nm with a mesopore diameter of 2 to 3 nm. An average mesopore size of 2.9 nm (Figure 1c) and a specific surface area of 999 m^2 g^{-1} (Figure 1d) for the as-synthesized MSN were observed by BJH and BET analysis, respectively. The continuous functionalization of MSN was confirmed by FT–IR. After removal of *N*-cetyltrimethylammonium bromide (CTAB) from the CTAB@MSN, the interior and exterior surfaces of the obtained MSN were functionalized with 3-mercaptopropyltrimethoxysilane to prepare MSN-SH. A thiol absorption band at 2600 cm^{-1} from the FT–IR spectrum of MSN-SH (Figure S5) confirmed the successful modification. Thereafter, CPT@MSN-hyd-DOX was fabricated via a one-pot strategy, and DOX was anchored onto the MSN surface by MSN-SH reacting with Mal-hyd-DOX during the loading course of CPT. All of the other nanoparticles used as controls were prepared with a similar procedure.

As shown in Figure 1b, the morphology and shape of CPT@MSN-hyd-DOX did not change significantly, indicating that the nanoparticles can retain their morphology after CPT loading and DOX conjugating. However, the mesopore arrays on the CPT@MSN-hyd-DOX nanoparticles almost disappeared. Thermal gravimetric analysis was utilized to confirm further the successful preparation of the CPT@MSN-hyd-DOX nanoparticles. When the temperature was increased to 800 °C, the weight loss values of MSN and CPT@MSN-hyd-DOX were 15.0 and 17.0% (Figure 2), respectively. The increased

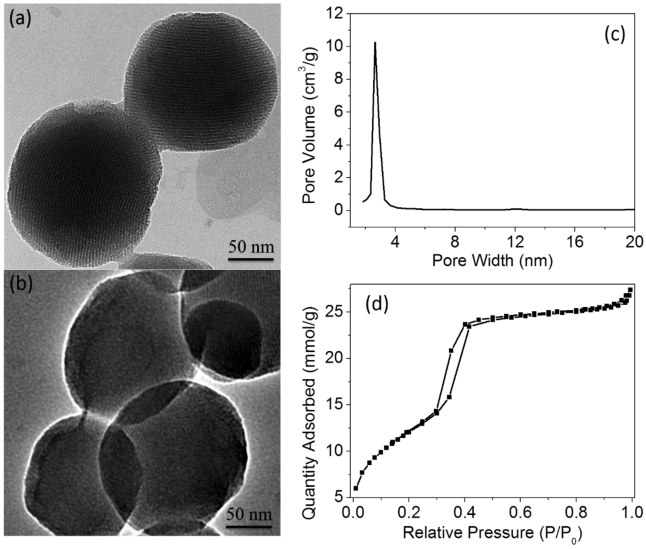

Figure 1. TEM images of MSN (a) and CPT@MSN-hyd-DOX (b), Barrett–Joyner–Halenda pore distribution (c), and nitrogen adsorption/desorption isotherms of MSN (d).

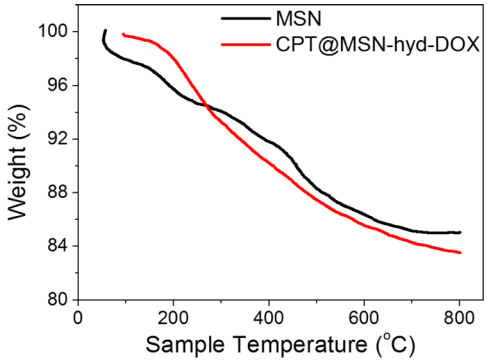

Figure 2. TGA curves of the different nanoparticles.

weight loss indicated that DOX was successfully immobilized onto the interior and exterior surfaces, whereas CPT was successfully loaded in the mesopores of the nanoparticles. After the nanoparticles with the indicated weight were dissolved in HF solution and neutralized by a 1 M NaOH solution, the drug-loading efficiency (DLE) of the nanoparticle was determined by fluorescence spectroscopy and the results are listed in Table 1 (DLE_{DOX}: 4.72% and DLE_{CPT}: 5.30% for CPT@MSN-hyd-DOX).

Controlled Drug Release. The degradation of the hydrazone bonds of CPT@MSN-hyd-DOX will result in the release of DOX from the nanoparticles. To verify the pH-sensitive release, we used fluorescence spectroscopy to quantitate the release behavior of DOX from CPT@MSN-hyd-DOX using CPT@MSN-urea-DOX as a control. The results shown in Figure 3a reveal a slow release of around 15% of DOX from CPT@MSN-hyd-DOX after 100 h at pH 7.4.

dx.doi.org/10.1021/am402082d | ACS Appl. Mater. Interfaces 2013, 5, 7995–8001

Table 1. Drug-Loading Efficiencies of the Nanoparticles

	CPT@MSN-hyd-DOX	CPT@MSN-urea-DOX	MSN-hyd-DOX	CPT@MSN	MSN-urea-DOX
DOX loading efficiency (%)	4.72	1.89	2.04		3.61
CPT loading efficiency (%)	5.30	2.12		2.67	

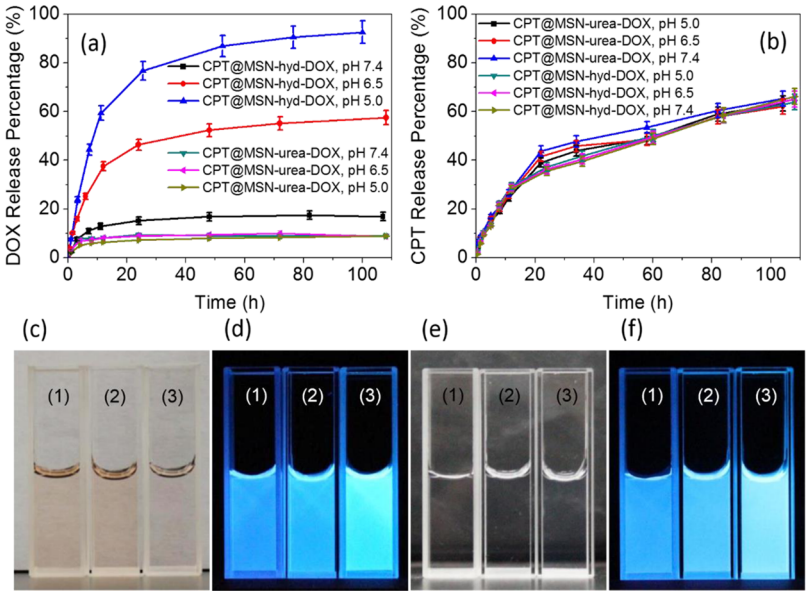

Figure 3. DOX (a) and CPT (b) release profiles of CPT@MSN-hyd-DOX and CPT@MSN-urea-DOX for different pH values. White-light (c, e) and fluorescent (d, f) images (λ_{ex} = 365 nm) of the supernatants after CPT@MSN-hyd-DOX (c, d) and CPT@MSN-urea-DOX (e, f) incubation for 6 h at pH 5.0 (1), 6.5 (2), and 7.4 (3).

However, a much faster release of DOX was observed when CPT@MSN-hyd-DOX was incubated at pH 6.5, and about 55% of DOX was released after 100 h. To simulate DOX release within endosomes and lysosomes, CPT@MSN-hyd-DOX was further incubated at pH 5.0. As shown in Figure 3a, over 60% of DOX was released in 10 h, and 90% of DOX was released after 100 h of incubation. Obviously, DOX could be rapidly freed from CPT@MSN-hyd-DOX, and the release adopted a burst mode under endo/lysosomal conditions, which makes it possible to effectively terminate malignant cells during cancer therapy. As expected, the release of DOX from the control, CPT@MSN-urea-DOX, was negligible. The cumulative release of DOX from CPT@MSN-urea-DOX was less than 8% over 100 h (Figure 3a). Meanwhile, the release rate was independent of the pH of the media. To examine whether the release of CPT from nanoparticles also adopts the pH-responsive manner, fluorescence spectroscopy was utilized to quantitatively determine the CPT release. The results shown in Figure 3b indicate that both the CPT@MSN-hyd-DOX and CPT@MSN-urea-DOX nanoparticles exhibited similar sustained CPT release for more than 100 h at different pH values. CPT release from the two types of nanoparticles was almost independent of pH variations. In addition, CPT and DOX release did not interfere with each other at each indicated pH condition.

From the white-light observation, a slightly orange supernatant was observed after 6 h of incubation of CPT@MSN-hyd-DOX at pH 7.4 (Figure 3c3). However, incubation of the same specimen at pH 5.0 for 6 h resulted in a cloudy orange supernatant (Figure 3c1) that was a little bit deeper in color than that at pH 6.5 (Figure 3c2). The observed color can be assigned to the released DOX because the released CPT was invisible in buffer solutions (Figure S6e). The data demonstrate that the cleavage of the hydrazone linkers was accelerated at lower pH values. Additionally, MSN-hyd-DOX was used to visually verify that DOX can be selectively released at pH 6.5 or 5.0. It was found that almost no discernible DOX was released at neutral pH (Figure S6b3). At the lyso/endosomal pH, however, most DOX molecules were cleaved from the MSN-hyd-DOX (Figure S6b1), which was slightly larger than that under the acidity of tumor cellular compartments (pH 6.5, Figure S6b2). To substantiate further that acidic pH values cannot trigger the release of DOX for MSN-urea-DOX (DOX can be stabilized within MSN-urea-DOX at the experimental pH values), we studied the centrifugal MSN-urea-DOX with DOX fluorescence (excited at 365 nm) and no DOX was released either at neutral or acidic pH (Figure S6d). From the white-light images of CPT@MSN-urea-DOX, a clear supernatant was observed after a 6 h incubation at three different pH values (Figure 3e). The results were consistent with the fact that the urea linker was not an acid-labile bond, which was stable at all of the experimental pH values. When CPT@MSN-hyd-DOX and CPT@MSN-urea-DOX were incubated separately for 6 h at three different pH values, we also observed that the centrifugal samples were excited at 365 nm. Interestingly, there was a similar pattern between them (Figure 3d,f), which was attributed to the strong fluorescence from CPT excited by the UV lamp. It is worth noting that the pH variations induced the CPT fluorescent differences seen in Figure 3d1−d3 (also confirmed by Figure S6f).

Cytotoxicity, Combination Index, and Synergism Analysis. Cytotoxicity was evaluated by MTT assay against U87 MG cells after different treatments for 48 h. No apparent toxicity was observed for MSN. Even at a high concentration of

400 μg mL^{-1}, the cell viability was still as high as 88% (Figure 4c). According to the literature,[27] MSN is able to transport and

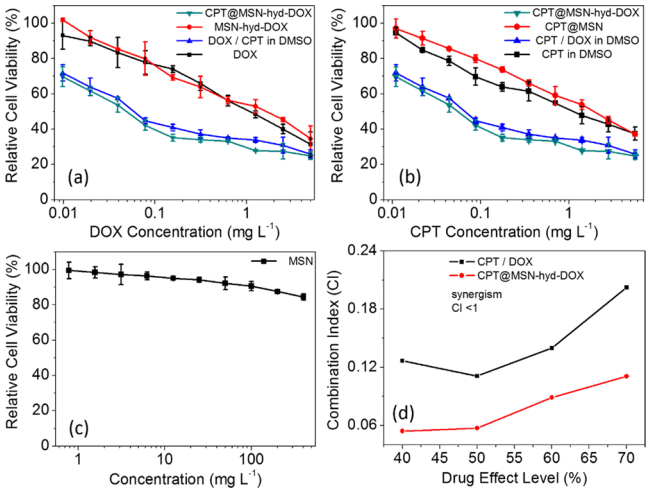

Figure 4. Viability of U87 MG cells incubated with DOX, CPT (in DMSO), DOX/CPT (in DMSO), MSN-hyd-DOX, CPT@MSN, CPT@MSN-hyd-DOX, and MSN at different doses (a–c). Combination index (CI) of DOX/CPT combinations via different modes of delivery (d).

deliver hydrophobic anticancer drugs such as CPT into cancer cells, leading to growth inhibition and cell death. As shown in Figure 4b, CPT@MSN and CPT (in DMSO) exhibited significant and very similar cytotoxicity against U87 MG cells. By contrast, CPT suspended in PBS showed negligible cytotoxicity (data not shown). This is consistent with the literature observation that CPT suspended in PBS cannot be taken up by tumor cells because of its insolubility in PBS.[27]

To overcome the rapid development of drug resistance in tumor cells, anticancer drugs without cross-resistance are always used together in clinical chemotherapy. Herein, DOX was conjugated to the nanoparticles via the acid-labile hydrazone bond, and CPT was loaded in the MSN pores to prepare CPT@MSN-hyd-DOX. It was found that the cell-inhibition effect of CPT@MSN-hyd-DOX was much greater than that of CPT@MSN (Figure 4a,b) because of the conspicuous synergistic effect between DOX and CPT. Herein, the combination index (CI), which could provide qualitative information on the drug interaction nature, is calculated from the following equation[29,30]

$$\mathrm{CI} = \frac{D_{\mathrm{A}}}{D_{\mathrm{mA}}} + \frac{D_{\mathrm{B}}}{D_{\mathrm{mB}}}$$

where D_{A} and D_{B} are the concentrations of drug A and drug B, respectively, that function in combination to achieve a specified drug effect (e.g., 50% inhibition of cell viability). D_{mA} and D_{mB} are the doses for single drugs to achieve the same effect. A CI value of less than, equal to, and more than 1 indicates synergism, additivity, and antagonism, respectively. When the CI values are plotted versus the drug-effect levels (ICx values), quantitative information on the nature and extent of drug interactions could be provided.[29,30] As shown in Figure 4d, the CI values of both the CPT/DOX mixture and CPT@MSN-hyd-DOX were far lower than 1 at the drug-effect levels ranging from 40 to 70%, displaying a remarkable synergistic effect between CPT and DOX. In addition, the CI value of CPT@MSN-hyd-DOX was even lower than that of the CPT/DOX mixture at each corresponding drug-effect level. In other words, the synergistic effect became more apparent by loading the drugs into the MSNs. The result can be explained by the DOX-conjugated nanoparticles loaded with CPT being easily taken up by the cancer cells as well as the drugs being effectively released from the nanoparticles with effective synergistic therapy. Because the synergism correlates with the DOX release, it was hypothesized that the acid-labile hydrazone bond for DOX immobilization in CPT@MSN-hyd-DOX did play an irreplaceable role in the synergism that occurred between DOX and CPT. To demonstrate this further, two nanoparticles, MSN-urea-DOX and CPT@MSN-urea-DOX, were fabricated by immobilizing DOX onto the nanoparticles via an acid-stable urea linkage as the controls. As mentioned above, DOX is hardly released from CPT@MSN-urea-DOX (Figure 3a) and MSN-urea-DOX (data not shown).

As shown in Figure 5, MSN-urea-DOX exhibited a slight cell toxicity, and the toxicity was most likely generated by slight DOX leakage. On the contrary, MSN-hyd-DOX induced significant cell death at an equal DOX dosage. Meanwhile, CPT@MSN-urea-DOX was more toxic than MSN-urea-DOX (Figure 5a), which indicated that the increased toxicity derived from the CPT release.

It was reported that the tumor microenvironment is mildly acidic with a pH range of 5.8–7.1.[19] Because DOX release from CPT@MSN-hyd-DOX was accelerated at lower pH values, we tried to verify whether the toxicity from CPT@MSN-hyd-DOX adopted a "tumor-triggered" manner. From Figure 6, the U87 MG cell viability of CPT@MSN-hyd-DOX was ~70% at a concentration of 6.4 μg mL^{-1} (containing ~0.3 μg mL^{-1} of DOX and ~0.34 μg mL^{-1} of CPT) at pH 7.4 (Figure 6a). However, the cell viability decreased dramatically to around

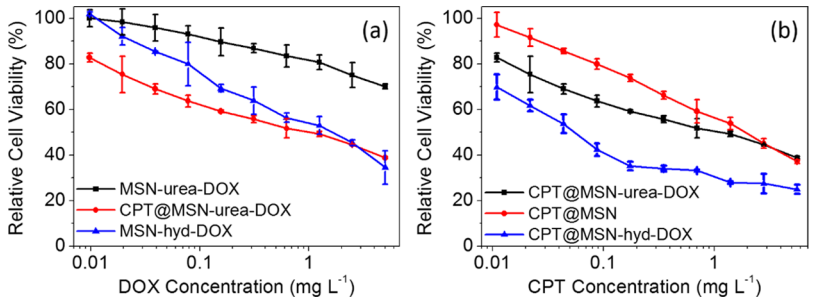

Figure 5. Viability of U87 MG cells incubated with MSN-hyd-DOX, MSN-urea-DOX, CPT@MSN, CPT@MSN-hyd-DOX, and CPT@MSN-urea-DOX at different doses (a, b).

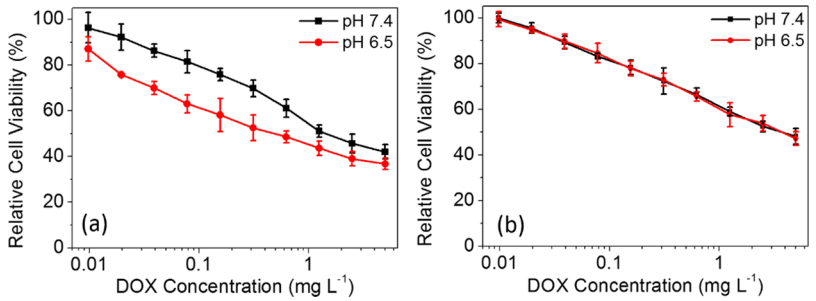

Figure 6. Viability of U87 MG cells incubated with CPT@MSN-hyd-DOX (a) and CPT@MSN-urea-DOX (b) at the indicated pH values.

50% at the same concentration when the medium pH was changed to 6.5 (Figure 6a). This decrease may attribute to the faster release of DOX under the acidic condition, although the difference in toxicity became smaller with the higher DOX dosage. When the cells were incubated with CPT@MSN-urea-DOX at the same DOX concentration, we did not find a similar effect (Figure 6b). Thus, the results demonstrate that the toxicity enhancement of CPT@MSN-hyd-DOX could be triggered by tumor microenvironment acidity. In other words, CPT@MSN-hyd-DOX could be "activated" by tumor-acidity for use in synergistic chemotherapy.

Intracellular Uptake. To observe the intracellular uptake and drug-release behavior, CPT@MSN-hyd-DOX or CPT@MSN-urea-DOX was added to U87 MG cells. After a 2 h incubation, the internalized nanoparticles were found to be initially localized in the acidic organelles (Figure S7), as evidenced by the yellow spots in the overlapped image of the red DOX and green LysoSensor stained lysosomes.

In another experiment, we incubated CPT@MSN-hyd-DOX with U87 MG cells for 4 h. The confocal laser-scanning microscope (CLSM) image in Figure 7 indicated that after a 4 h incubation, red fluorescence from DOX was partly localized in the nuclei of cells labeled with nuclear yellow (Figure 7). According to literature, mesoporous silica nanoparticles with a diameter over 100 nm can not transport across the nuclear membrane even with the help of a TAT peptide.[31] Over 25% of cumulative DOX was released from CPT@MSN-hyd-DOX at endo/lysosomal pH in 4 h, indicating that the internalized CPT@MSN-hyd-DOX could release DOX rapidly in response to the acidic environment of cancer cells, and the released DOX could partly diffuse into the nuclei of cells in 4 h. However, a similar phenomenon could not be observed for CPT@MSN-urea-DOX after a 4 h incubation with U87 MG cells. Additionally, the red fluorescence from CPT@MSN-hyd-DOX after a 4 h incubation with U87 MG cells was apparently stronger than that of CPT@MSN-urea-DOX. From these results, it was found that DOX could be released from CPT@MSN-hyd-DOX in response to the intracellular acidic microenvironment during or after their accumulation in U87 MG cells.

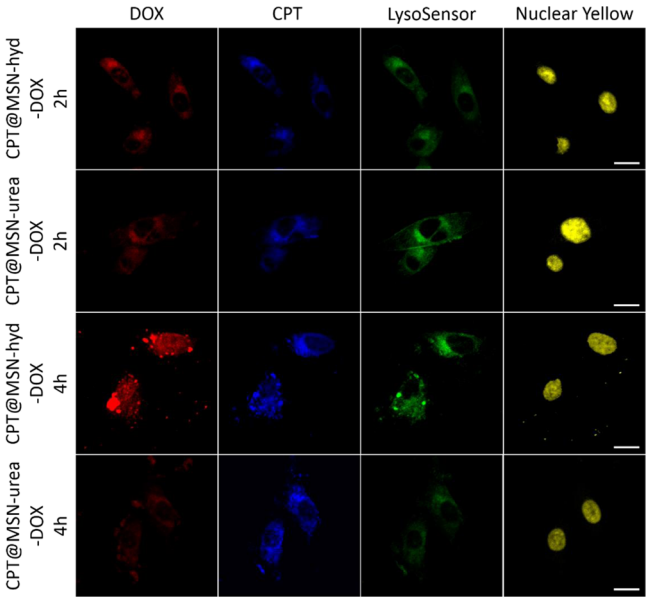

Figure 7. CLSM images of U87 MG cells treated with CPT@MSN-hyd-DOX or CPT@MSN-urea-DOX for 2 and 4 h. LysoSensor (green) was used to stain the acidic organelles of the cell, and nuclear yellow was used to stain the nuclei. Scale bar = 15 μm.

As for CPT release, it followed the free diffusion manner, and there was no remarkable difference between CPT@MSN-hyd-DOX and CPT@MSN-urea-DOX, which corresponds well with the above-mentioned CPT release. In addition, there was no discernible CPT detected in the nuclear region after a 4 h cell incubation with either CPT@MSN-hyd-DOX or CPT@MSN-urea-DOX.

CONCLUSIONS

A novel intelligent drug-delivery system, CPT@MSN-hyd-DOX, was constructed via a facile one-pot strategy, which exhibited tumor-acidity-activated synergistic chemotherapy against tumor cells. The nanoparticles could deliver CPT and DOX simultaneously into cancer cells and maintain a relatively "stealth" character during circulation. Because the tumor microenvironment is mildly acidic (around pH 6.5), this drug-delivery system could respond to tumors to realize tumor-acidity-activated synergistic chemotherapy. CPT@MSN-hyd-DOX, demonstrated here, could find great potential for use in the synergistic chemotherapy of glioblastoma.

ASSOCIATED CONTENT

Supporting Information

Synthesis of Mal-hyd-DOX; ^{1}H NMR spectra of 6-maleimidocaproic acid, 6-maleimidocaprohydrazide trifluoroacetic acid salt, and Mal-hyd-DOX; ESI−MS spectrum of Mal-hyd-DOX; FT−IR spectra of CTAB@MSN, MSN, MSN-SH, and CPT@MSN-hyd-DOX; white-light and fluorescent images of the supernatants after MSN-hyd-DOX, MSN-urea-DOX, CPT@MSN, and CPT@MSN-urea-DOX incubation for 6 h at different pHs; and confocal microscopy of the U87 MG cellular-uptake behavior of CPT@MSN-hyd-DOX and CPT@MSN-urea-DOX. This material is available free of charge via the Internet at http://pubs.acs.org.

AUTHOR INFORMATION

Corresponding Author

*E-mail: xz-zhang@whu.edu.cn.

Notes

The authors declare no competing financial interest.

ACKNOWLEDGMENTS

We acknowledge the financial support from the National Natural Science Foundation of China (51125014 and 51233003), the Ministry of Science and Technology of China (2011CB606202), and the Fundamental Research Fund for the Central Universities (201120302020007).

REFERENCES

(1) Clarke, J.; Butowski, N.; Chang, S. *Arch. Neurol.* **2010**, *67*, 279−283.
(2) Sorensen, A. G.; Batchelor, T. T.; Wen, P.; Zhang, W. T.; Jain, R. K. *Nat. Rev. Clin. Oncol.* **2008**, *5*, 634−644.
(3) DeVita, V. T., Jr.; Young, R. C.; Canellos, G. P. *Cancer* **1975**, *35*, 98−110.
(4) Shah, M. A.; Schwartz, G. K. *Drug Resist. Updates* **2000**, *3*, 335−356.
(5) Pavillard, V.; Kherfellah, D.; Richard, S.; Robert, J.; Montaudon, D. *Br. J. Cancer* **2001**, *85*, 1077−1083.
(6) Shen, Y. Q.; Jin, E. L.; Zhang, B.; Murphy, C. J.; Sui, M. H.; Zhao, J.; Wang, J. Q.; Tang, J. B.; Fan, M. H.; Van Kirk, E. W.; Murdoch, J. *J. Am. Chem. Soc.* **2010**, *132*, 4259−4265.
(7) Schmid, B.; Chung, D. E.; Warnecke, A.; Fichtner, I.; Kratz, F. *Bioconjugate Chem.* **2007**, *18*, 702−716.
(8) Saha, S.; Leung, K. C. F.; Nguyen, T. D.; Stoddart, J. F.; Zink, J. I. *Adv. Funct. Mater.* **2007**, *17*, 685−693.
(9) Rosenholm, J. M.; Sahlgren, C.; Linden, M. *Nanoscale* **2010**, *2*, 1870−1883.
(10) Torney, F.; Trewyn, B. G.; Lin, V. S. Y.; Wang, K. *Nat. Nanotechnol.* **2007**, *2*, 295−300.
(11) Liu, R.; Zhao, X.; Wu, T.; Feng, P. *J. Am. Chem. Soc.* **2008**, *130*, 14418−14419.
(12) Nguyen, T. D.; Liu, Y.; Saha, S.; Leung, K. C. F.; Stoddart, J. F.; Zink, J. I. *J. Am. Chem. Soc.* **2007**, *129*, 626−634.
(13) Kim, H.; Kim, S.; Park, C.; Lee, H.; Park, H. J.; Kim, C. *Adv. Mater.* **2010**, *22*, 4280−4283.
(14) Zhao, Y. L.; Li, Z.; Kabehie, S.; Botros, Y. Y.; Stoddart, J. F.; Zink, J. I. *J. Am. Chem. Soc.* **2010**, *132*, 13016−13025.
(15) Meng, H.; Xue, M.; Xia, T.; Zhao, Y. L.; Tamanoi, F.; Stoddart, J. F.; Zink, J. I.; Nel, A. E. *J. Am. Chem. Soc.* **2010**, *132*, 12690−12697.
(16) Park, C.; Lee, K.; Kim, C. *Angew. Chem., Int. Ed.* **2009**, *48*, 1275−1278.
(17) Schlossbauer, A.; Kecht, J.; Bein, T. *Angew. Chem., Int. Ed.* **2009**, *48*, 3092−3095.
(18) Bernardos, A.; Aznar, E.; Marcos, M. D.; Martínez-Máñez, R.; Sancenón, F.; Soto, J.; Barat, J. M.; Amorós, P. *Angew. Chem., Int. Ed.* **2009**, *48*, 5884−5887.
(19) Mok, H.; Veiseh, O.; Fang, C.; Kievit, F. M.; Wang, F. Y.; Park, J. O.; Zhang, M. *Mol. Pharmaceutics* **2010**, *7*, 1930−1939.
(20) Padilla-Parra, S.; Matos, P. M.; Kondo, N.; Marin, M.; Santos, N. C.; Melikyan, G. B. *Proc. Natl. Acad. Sci. U.S.A.* **2012**, *109*, 17627−17632.
(21) Zhang, Q.; Liu, F.; Nguyen, K. T.; Ma, X.; Wang, X. J.; Xing, B. G.; Zhao, Y. L. *Adv. Funct. Mater.* **2012**, *22*, 5144−5156.
(22) Park, C.; Oh, K.; Lee, S. C.; Kim, C. *Angew. Chem., Int. Ed.* **2007**, *46*, 1455−1457.
(23) Angelos, S.; Khashab, N. M.; Yang, Y. W.; Trabolsi, A.; Khatib, H. A.; Stoddart, J. F.; Zink, J. I. *J. Am. Chem. Soc.* **2009**, *131*, 12912−12914.
(24) Liu, R.; Zhang, Y.; Zhao, X.; Agarwal, A.; Mueller, L. J.; Feng, P. Y. *J. Am. Chem. Soc.* **2010**, *132*, 1500−1501.
(25) Gullotti, E.; Yeo, Y. *Mol. Pharmaceutics* **2009**, *6*, 1041−1051.
(26) Du, J. Z.; Sun, T. M.; Song, W. J.; Wu, J.; Wang, J. *Angew. Chem., Int. Ed.* **2010**, *49*, 3621−3626.
(27) Lu, J.; Liong, M.; Zink, J. I.; Tamanoi, F. *Small* **2007**, *3*, 1341−1346.
(28) Willner, D.; Trail, P. A.; Hofstead, S. J.; King, H. D.; Lasch, S. J.; Braslawsky, G. R.; Greenfield, R. S.; Kaneko, T.; Firestone, R. A. *Bioconjugate Chem.* **1993**, *4*, 521−527.
(29) Chou, T. C. *Cancer Res.* **2010**, *70*, 440−446.
(30) Xiao, H. H.; Li, W. L.; Qi, R. G.; Yan, L. S.; Wang, R.; Liu, S.; Zheng, Y. H.; Xie, Z. G.; Huang, Y. B.; Jing, X. B. *J. Controlled Release* **2012**, *163*, 304−314.
(31) Pan, L. M.; He, Q. J.; Liu, J. N.; Chen, Y.; Ma, M.; Zhang, L. L.; Shi, J. L. *J. Am. Chem. Soc.* **2012**, *134*, 5722−5725.